

Supporting Information

Properties of parallel tetramolecular G-quadruplex carrying N-acetylgalactosamine as potential enhancers for oligonucleotide delivery to hepatocytes.

Anna Clua^{1,2}, Santiago Grijalvo^{1,2}, Namrata Erande³, Swati Gupta³, Kristina Yucius³, Raimundo Gargallo⁴, Stefania Mazzini⁵, Muthiah Manoharan³, and Ramon Eritja^{1,2,*}

¹Institute for Advanced Chemistry of Catalonia (IQAC-CSIC), Jordi Girona 18-26, E-08034 Barcelona, Spain; acvtnt@cid.csic.es (A.C.); sgrgma@cid.csic.es (S.G.) ²Networking Center on Bioengineering, Biomaterials and Nanomedicine (CIBER-BBN), E-08034 Barcelona ³Alnylam Pharmaceuticals, 300 Third Street, Cambridge, Massachusetts 02142, United States; nd.erande@gmail.com (N.E.); sgupta@alnylam.com (S.G.); kyucius@alnylam.com (K.Y.); mmanoharan@alnylam.com (M.M.) ⁴University of Barcelona, Department of Chemical Engineering and Analytical Chemistry, Martí i Franquès 1-11, E-08028 Barcelona, Spain; raimon_gargallo@ub.edu (R.G) ⁵Università degli Studi di Milano, DEFENS-Dipartimento Di Scienze per Gli Alimenti, la Nutrizione e l'Ambiente, Via Celoria, 2 Italia-20133, Milano, Italy; stefania.mazzini@unimi.it (S.M.)

Corresponding Author

* Email; recgma@cid.csic.es (R. E).

Table of contents:

| | |
|---|--------|
| 1. Figure S1. Schematic representation of the potential tetrameric G-quadruplexes. | Page 3 |
| 2. Table S1. Sequences and mass spectra of oligonucleotide derivatives prepared in this work.. | Page 4 |
| 3. Table S2. Oligonucleotide RNA derivatives carrying anti-mTTR siRNA sequence. | Page 4 |
| 4. Figure S2. Melting curves on G-quadruplex sequence (G-PO-HCV-L235). | Page 5 |
| 5. Figure S3. CD spectra of G-rich and control oligonucleotides | Page 6 |
| 6. Figure S4. Analysis of stability of G-rich oligonucleotides to FBS and phosphodiesterase. | Page 7 |
| 7. Figure S5. MTT assay in HeLa (a), and HepG2 (b) cells. | Page 9 |

Figure S1. Schematic representation of the potential tetrameric G-quadruplexes carrying four GalNAc molecules by tetramerization of monofunctionalized GalNAc G-rich oligonucleotide. **I.** Tetravalent GalNAc linked to HVC sequence (H series, Table 1). **II.** Tetravalent GalNAc linked to antisense oligonucleotide (Gapmer, L series, Table 2). **III.** Tetravalent GalNAc linked to an siRNA (R series, Table S2). The study shows that structures I and II can be observed and may be responsible of an increased affinity to ASGPR and an increased antisense activity in hepatocytes while structure III most probably is not formed.

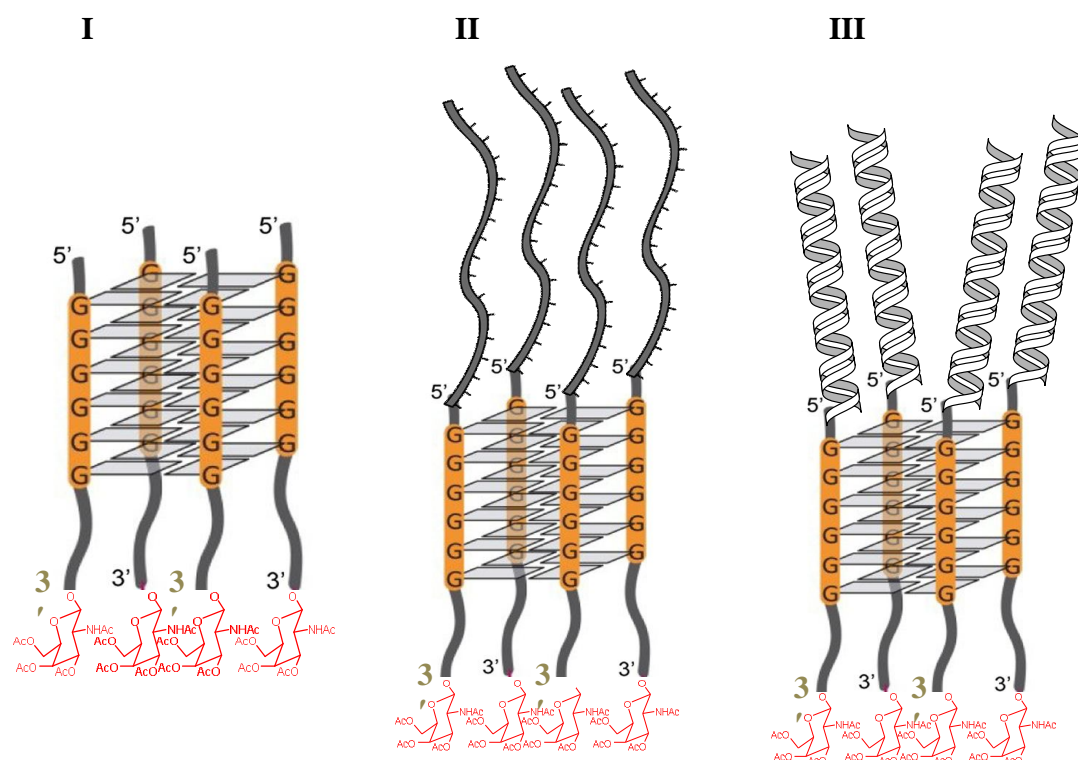


Table S1. Sequences and Mass spectra of Oligonucleotide derivatives prepared in this work.

| N | Name | Sequence (5'-3') | MW Exp. | MW Found |
|-----|--------------------------------|--|---------|-----------------------|
| H1 | control | TTGGGGGGTACAGTGCA | 5304 | 5295 |
| H2 | G-PO-HCV-L235 | TTGGGGGGTACAGTGCA-L235 | 5786 | 5776 |
| H3 | A-PO-HCV-L235 | TTGAAAGGTACAGTGCA-L235 | 5738 | 5727 |
| H4 | G-PO-HCV-L193 | TTGGGGGGTACAGTGCA-L193 | 5885 | 5889 |
| H5 | A-PO-HCV-L193 | TTGAAAGGTACAGTGCA-L193 | 5837 | 5841 |
| H6 | FAM-G-PO-HCV-L235 | FAM-TTGGGGGGTACAGTGCA-L235 | 6353 | 6342 |
| H7 | FAM-G-PO-HCV-L193 | FAM-TTGGGGGGTACAGTGCA-L193 | 6452 | 6454 |
| H8 | A-PS-HCV-L235 | TsTsGAAAGGTACAGsTsGsCsA-L235 | 5834 | 5824 |
| H9 | A-PS-HCV-L193 | TsTsGAAAGGTACAGsTsGsCsA-L193 | 5933 | 5936 |
| H10 | G-PS-HCV-L235 | TsTsGGGGGGTACAGsTsGsCsA-L235 | 5885 | 5872 |
| H11 | G-PS-HCV-L193 | TsTsGGGGGGTACAGsTsGsCsA-L193 | 5981 | 5986 |
| H12 | A-PO-HCV-L96 | TTGAAAGGTACAGTGCA-L96 | 7043 | nd |
| L1 | ASO control | CsGsTsTsTsCsCsTsTsTsGsTsTsCsTsGsGsA | 5732 | 5720 |
| L2 | Gapmer control | <u>CsGsUsUsTsCsCsTsTsTsGsTsTsCsUsGsGsA</u> | 5912 | 5920 |
| L3 | Luc_G ₆ _GalNAc | <u>CsGsUsUsTsCsCsTsTsTsGsTsTsCsUsGsGsA</u> T GGGGGGT-L193 | 9075 | Broad 9200 (M+nNa) |
| L4 | G ₆ _Luc_GalNAc | TGGGGGGT <u>CsGsUsUsTsCsCsTsTsTsGsTsTsCsUsGsGsA</u> -L193 | 9075 | 9115 (M+2Na) |
| L5 | Luc_T_GalNAc | CGUUTCCTTTGTTCUGGATTTT-L193 | 7773 | 7728 / 7770 |
| L6 | Scr_Luc_G ₆ _GalNAc | <u>CsUsGsUsCsTsGsAsCsGsTsTsCsTsUsUsGsUs</u> TGGGGGGT-L193 | 9055 | Broad 9500 (M+nNa) |
| L7 | FAM_Luc_G ₆ _GalNAc | FAM- <u>CsUsGsUsTsCsCsTsTsTsGsTsTsCsUsGsGsA</u> T TGGGGGGT-L193 | 9642 | Broad 9800 (M+nNa) |
| L8 | T ₈ | TTTTTTTT | 2370 | 2365 |

nd: not determined. “s” indicate the position of the phosphorothioate linkages. Underlined nucleotides indicate 2'-O-methyl-RNA derivatives

Table S2. Oligonucleotide RNA derivatives carrying anti-mTTR siRNA sequence. Small letters (a, u, g, c) indicate 2'-O-Me nucleotide; capital letters with F (Af, Uf, Gf, Cf) indicate 2'-fluororibonucleotide; capital letters (A, G, U, C) indicate RNA nucleotides; capital letters with d in (dA, dT, dG, dC) indicate 2'-deoxy nucleotides; “s” in (as, us, gs, cs, Afs, Ufs, Gfs, Cfs, dAs) indicate the position of the phosphorothioate linkages.

| N | Name | Sequence (5'-3') | GalNAc |
|----|-------------------|---|--------|
| R1 | A117799 sense | Afs-as-Cf-a-Gf-u-Gf-u-Uf-Cf-Uf-u-Gf-c-Uf-c-Uf-a-Uf-a-Af-L96 | L96 |
| R2 | A1411192 sense | Afs-as-Cf-a-Gf-u-Gf-u-Uf-Cf-Uf-u-Gf-c-Uf-c-Uf-a-Uf-a-Af-dTdTdTdGdGdGdGdGdT-L193 | L193 |
| R3 | A117800 antisense | Us-Ufs-a-Uf-a-Gf-a-Gf-c-Af-a-g-a-Af-c-Af-c-Uf-g-Uf-us-us-u | --- |

Figure S2. Melting curves on G-rich sequence H2 (G-PO-HCV-L235). CD spectra shows minor changes with increasing temperature. The CD signal at 265 nm does not change with increasing temperature up to 90 °C. The same results were found for the G-rich sequences H4 (G-PO-HCV-L193), H10 (G-PS-HCV-L235) and H11 (G-PS-HCV-L193). Working concentration (5 μ M) in 10 mM lithium cacodylate buffer pH 7.2 supplemented with 0.11M NaCl. Samples were heated up to 90 °C. All studied G-rich oligonucleotides were stable up to 90 °C.

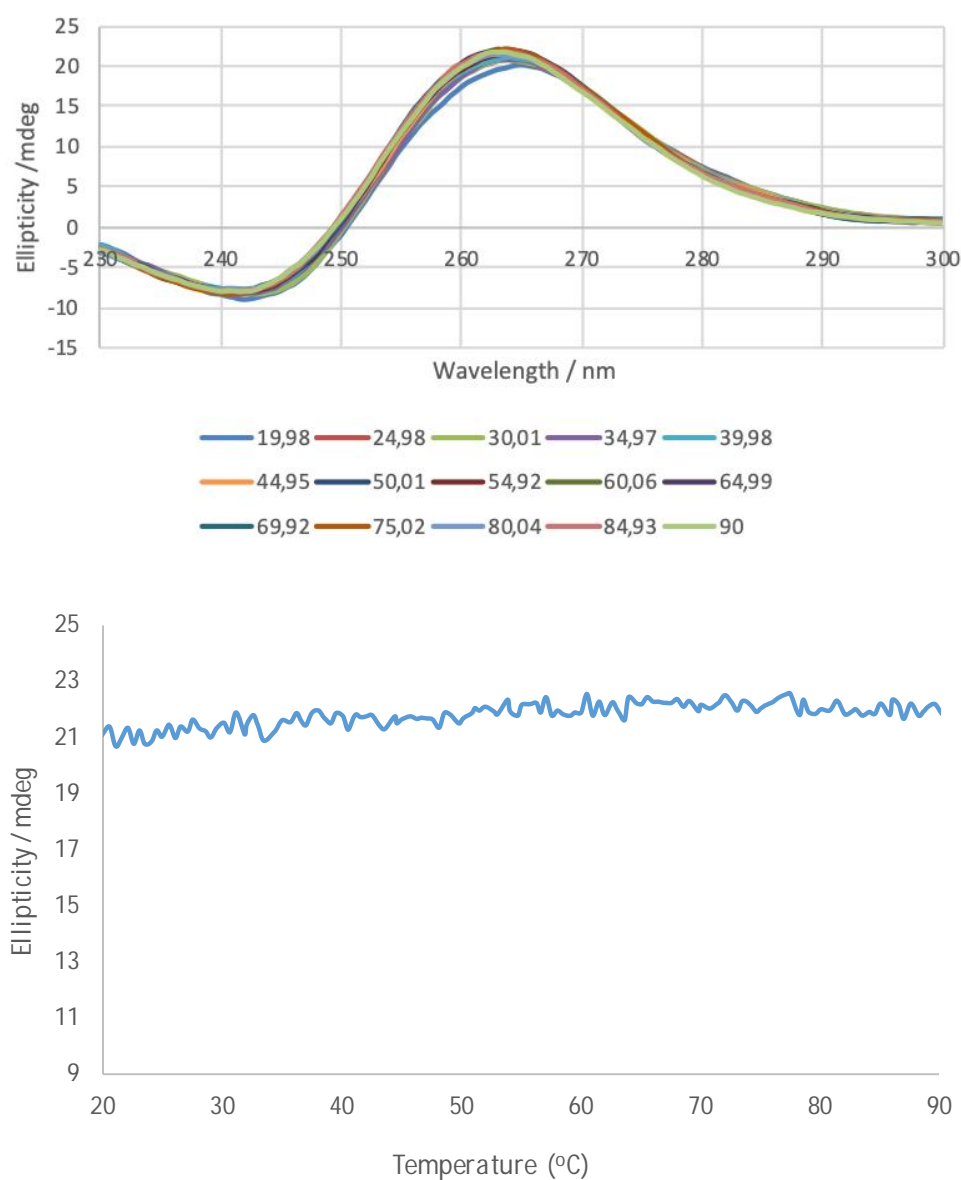
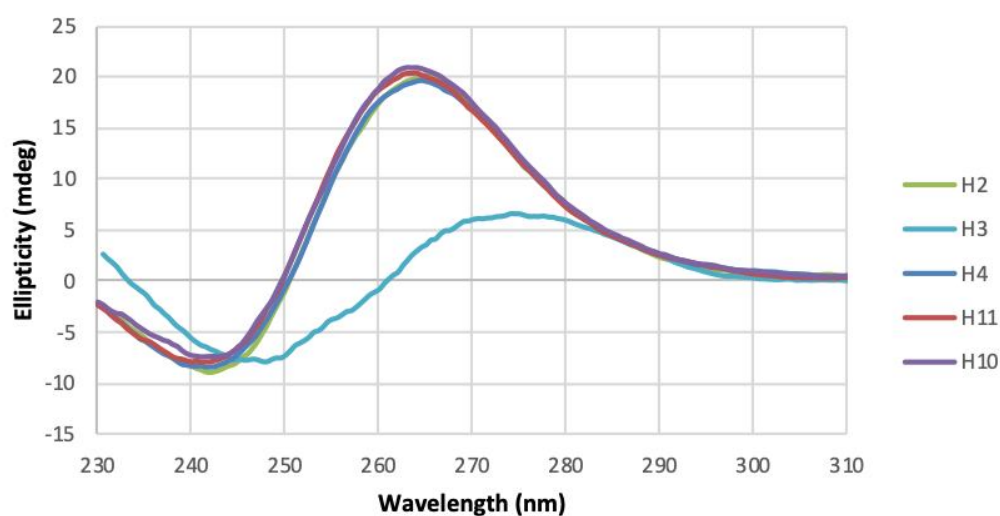


Figure S3. CD spectra of **A)** Oligonucleotides H2 (G-PO-HCV-L235), H3 (A-PO-HCV-L235), H4 (G-PO-HCV-L193), H10 (G-PS-HCV-L235), and H11 (G-PS-HCV-L193) and **B)** Oligonucleotides L3 (Luc_G₆_GalNAc), L4 (G₆_Luc_GalNAc), L5 (Luc_T₄_GalNAc), L6 (Scr_Luc_G₆_GalNAc). G-rich oligonucleotides show the maximum at 265 nm compared with non A-rich (H3) or T-rich (L5) control sequences that have the maximum at 275 nm. Working concentration (5 μ M) in PBS 1x.

A)



B)

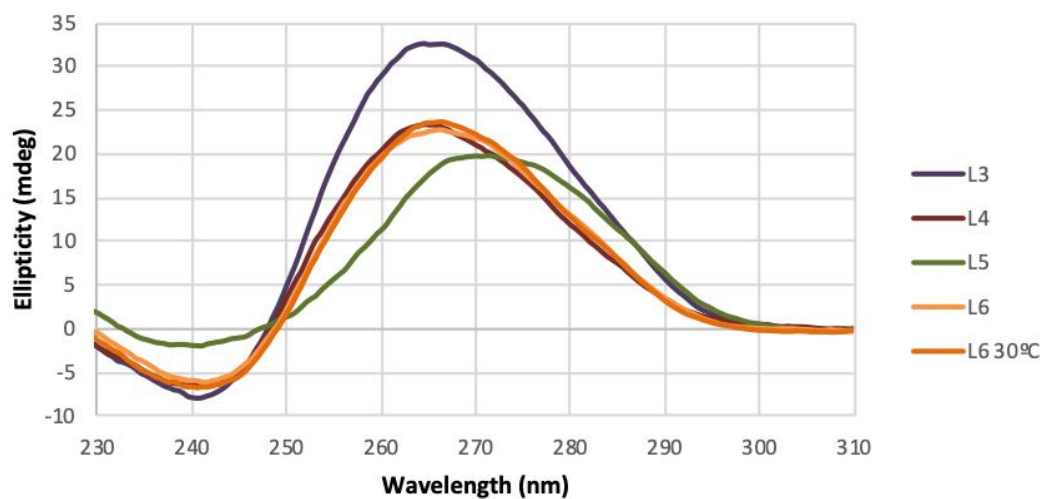


Figure S4. A. Analysis of stability of H6 (FAM-G-PO-HCV-L235) and H7 (FAM-G-PO-HCV-L193) G-rich oligonucleotides towards snake venom phosphodiesterase and 10% FBS (experimental conditions in cell studies). In snake venom phosphodiesterase, at 4 hr the spots corresponding to the full length H6 and H7 are clearly visible and disappeared between 8-24 hours. In 10% FBS two spots are seen: one having the mobility of the spots seen in snake venom phosphodiesterase that present a similar stability and a retarded band that may correspond to the oligonucleotide complexed with serum proteins that are unchanged over the time of incubation.

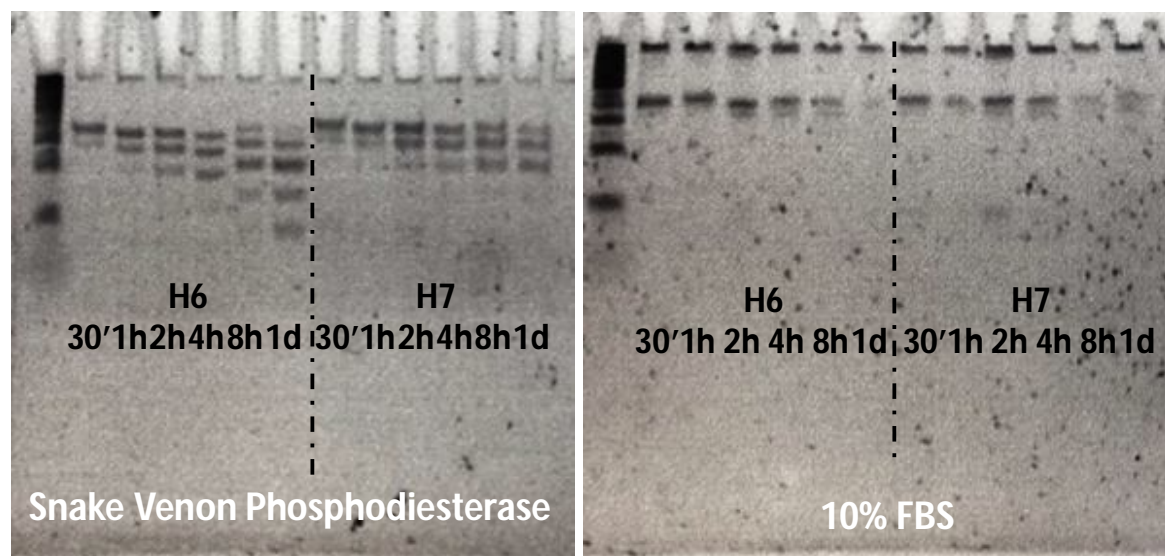


Figure S4. B. Analysis of stability of L4 (G₆-Luc-GalNAc) and L7 (FAM-Luc-G₆-GalNAc) G-rich oligonucleotides towards snake venom phosphodiesterase and 10% FBS (experimental conditions used in cell studies). In snake venom phosphodiesterase, the spots corresponding to the full length L4 and L7 are clearly visible after 24 hours confirming the stability of these highly modified oligonucleotides (gapmers with full phosphorothioate linkages). In 10% FBS only a main retarded band is seen that may correspond to the oligonucleotide complexed with serum proteins that are unchanged over the time of incubation. These data indicate that most probably these oligonucleotides carrying phosphorothioate and 2'-O-methyl residues bind to serum proteins that may protect the oligonucleotides from degradation.

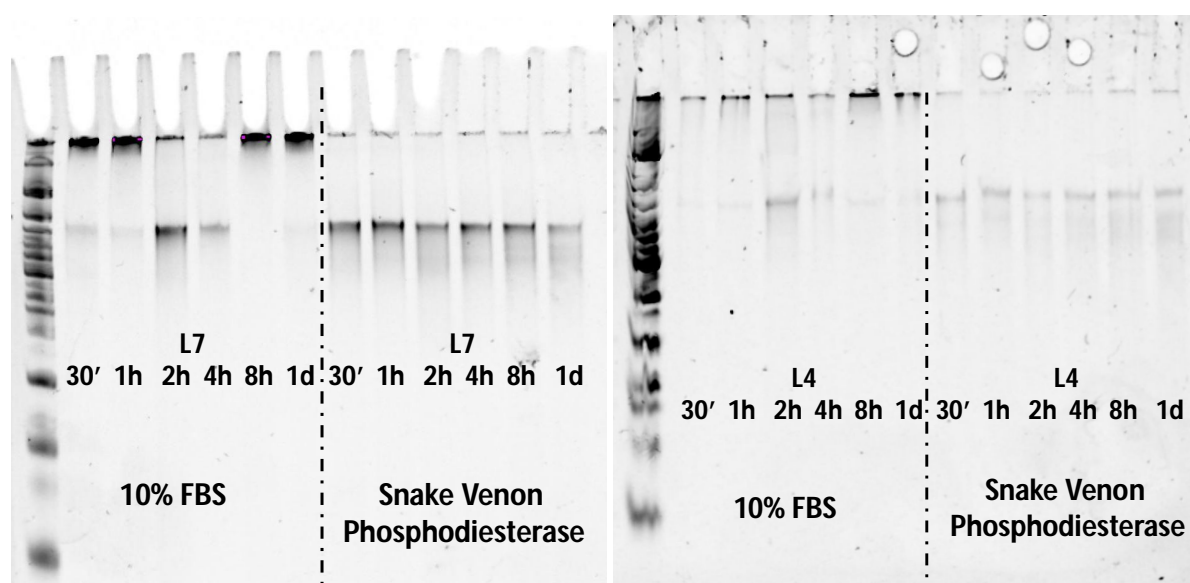
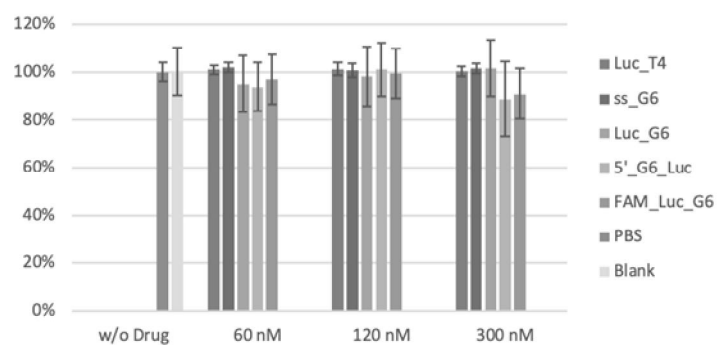


Figure S5. MTT assay in HeLa (a), and HepG2 (b) at 60, 120 and 300nM concentration of oligonucleotides. Luc_T₄_GalNAc (L5), Luc_G₆_GalNAc (L3), 5'-G₆_Luc_GalNAc (L4), FAM_Luc_G₆_GalNAc (L7).

a)



b)

